LA-UR-99-5452

## Inhomogeneous Low Frequency Spin Dynamics in La<sub>1.65</sub>Eu<sub>0.2</sub>Sr<sub>0.15</sub>CuO<sub>4</sub>

N.J. Curro, P.C. Hammel, B.J. Suh, A. Hücker, B. Büchner, U. Ammerahl, A. Revcolevschi Condensed Matter and Thermal Physics, Los Alamos National Laboratory, Los Alamos, NM 87545, USA
Division of Natural Science, The Catholic University of Korea, Korea

II. Physikalisches Institut, Universität zu Köln, Germany
Laboratoire de Chimie des Solides, Université Paris-Sud, 91405 Orsay Cedex, France
(Received:

We report Cu and La nuclear magnetic resonance (NMR) measurements in the title compound that reveal an inhomogeneous glassy behavior of the spin dynamics. A low temperature peak in the La spin lattice relaxation rate and the "wipeout" of Cu intensity both arise from these slow electronic spin fluctuations that reveal a distribution of activation energies. Inhomogeneous slowing of spin fluctuations appears to be a general feature of doped lanthanum cuprate.

PACS Numbers: 76.60.-k, 74.72.Bk, 75.30.Ds, 75.40.Gb

Lanthanum cuprate, the prototypical single layer high temperature superconductor, has been extensively studied for several years to understand the origin of its unusual normal state behavior as well as the mechanism for superconductivity. Rare earth co-doped lanthanum cuprate has received attention recently because elastic neutron scattering experiments have revealed ordering of doped holes into charged stripes that constitute antiphase domain walls producing incommensurate antiferromagnetic (AF) order in the intervening undoped domains [1]. Charge stripe order is likely intimately related to the high temperature superconductivity [2–5]. Isostructural lanthanum nickelate demonstrates clear stripe order [6]. and it has been shown there that both the charge order and the magnetic order are glassy [6,7]. It is also known that the magnetic order associated with charge ordering in lanthanum cuprate is glassy [8,9], but this situation is more difficult because the charge superlattice peaks are very hard to observe, presumably because the stripes tend to be dynamic. As a consequence little detail is known about the glassy behavior. Hunt et al. have observed suppression of the Cu NQR signal intensity ("wipeout") with decreasing temperature that they attribute to charge stripe order [10].

NMR provides information complementary to neutron scattering because the nuclei are sensitive to the local magnetic field and the dynamic behavior of the electronic system without requiring spatial correlations. Chou et al., first proposed that the very strong peak in the <sup>139</sup>La nuclear spin relaxation rate  $^{139}T_1^{-1}$  in the vicinity of T = 10 K is associated with spin freezing [11]. Kataev et al. have observed slow spin fluctuations in  $\text{La}_{1.8-x}\text{Eu}_{0.2}\text{Sr}_x\text{CuO}_4$  at low T [12]. Our single crystal studies of  $^{139}T_1^{-1}$  have shown that the peak is due to continuously slowing electronic spin fluctuations; in particular the characteristic fluctuation frequency  $\tau_c^{-1}$  displays an activated temperature dependence [13]. Furthermore, these data demonstrate a distribution  $P(E_a)$ of activation energies  $E_a$  centered at  $E_a/k_BT \sim 50 \text{ K}$ and with a width comparable this center value indicating strongly inhomogeneous magnetic properties [13]. To

understand if this inhomogeneity arises from disorder due to, e.g., substitutional dopants, we have applied this analysis to several lanthanum cuprate systems exhibiting AF order at low temperatures to allow us to explore the effect of varying the density and character of the disorder: in-plane doping by Li substitution for Cu, variation of doping density in LTT phase  $\text{La}_{1.8-x}\text{Eu}_{0.2}\text{Sr}_x\text{CuO}_4$ :  $0.01 \leq x \leq 0.15$ . Remarkably, we find that the character of the inhomogeneity, that is, the distribution of activation energies is essentially unchanged in all these cases and very similar to lightly doped  $\text{La}_{2-x}\text{Sr}_x\text{CuO}_4$  [11], suggesting that this inhomogeneity is *intrinsic* rather than arising from impurity disorder.

These inhomogeneous slow spin fluctuations also enhance the Cu spin relaxation rate  $^{63}T_1^{-1}$  and directly explain the wipeout of Cu intensity reported by Hunt et al. [10]. Because Cu nuclear moments experience a hyperfine coupling  $A_{\rm hf}$  to these fluctuations that is two orders of magnitude larger than for  $^{139}{\rm La}$  and  $^{63}T_1^{-1} \propto A_{\rm hf}^2$ ,  $^{63}T_1^{-1}$  becomes so fast as to relax the signal before it can be observed. The distribution of electron spin fluctuation frequencies means that different Cu spins will move out of the observation window of the spectrometer at different temperatures; using  $P(E_a)$  obtained from  $^{139}T_1^{-1}$  we obtain a quantitative explanation for the loss of Cu intensity.

Co-doping with J=0 Eu rather than Nd is advantageous: neither the magnetism in the CuO<sub>2</sub> plane nor the nuclear magnetism suffer the effects of the large Nd magnetic moment. The crystal used in this study was grown using the traveling solvent floating zone method under oxygen pressure of 3 bar [14]. Diffraction data as well as La NMR indicate a sharp LTT structural phase transition at  $135\pm2$  K. The observation of incommensurate magnetic peaks near 30 K in Eu co-doped compounds by elastic neutron scattering [15] reveals static magnetic stripe order. From dc magnetization measurements, no superconducting transition is observed down to 4.2K.  $\mu$ SR studies of this sample reveal static spin order below 25K [16].

The <sup>139</sup>La  $(I = \frac{7}{2})$  and <sup>63</sup>Cu  $(I = \frac{3}{2})$  NMR measure-

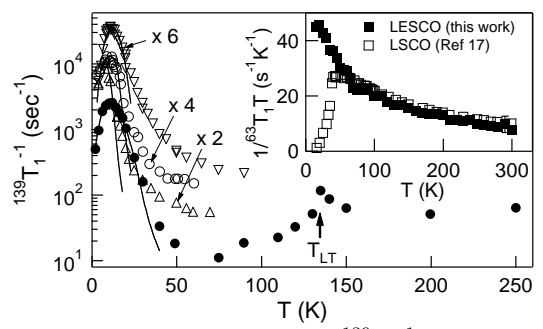


FIG. 1. T dependencies of  $^{139}T_1^{-1}$  in lanthanum cuprate doped by various routes:  $\text{La}_{1.65}\text{Eu}_{0.2}\text{Sr}_{0.15}\text{CuO}_4(\bullet)$ ,  $\text{La}_2\text{Cu}_{0.981}\text{Li}_{0.19}\text{O}_4$  ( $\bigtriangledown$ ),  $\text{La}_{1.8-x}\text{Eu}_{0.2}\text{Sr}_x\text{CuO}_4$  ( $\triangle$ ), and  $\text{La}_{1.986}\text{Sr}_{0.014}\text{CuO}_4$  ( $\bigcirc$ , from [11]). Solid lines are fits as described in the text using the parameters shown in Table 1. Inset:  $(^{63}T_1T)^{-1}$  versus T in  $\text{La}_{1.65}\text{Eu}_{0.2}\text{Sr}_{0.15}\text{CuO}_4$  (solid squares) and  $\text{La}_{1.85}\text{Sr}_{0.15}\text{CuO}_4$  (open squares; from [17]).

ments were made on the central  $(m_I = +\frac{1}{2} \leftrightarrow -\frac{1}{2})$  transition. The spin lattice relaxation rates were measured by monitoring the recovery of the magnetization after an inversion  $(\pi)$  pulse, and the echo decay of the Cu was observed by measuring the spin echo integral. The Cu spin lattice relaxation and echo decay data were measured in a field of 84.2 kG, and the La spin lattice relaxation data were obtained in a field of 59.7 kG. The intensities of the Cu and La signals were obtained from field swept spectra at constant frequency; the areas A under the spectra were then adjusted for echo decay and spin lattice relaxation effects.

 $^{139}T_1^{-1}$  is ideal for probing slow electron spin fluctuations because La is located outside of the CuO<sub>2</sub> planes, and so only weakly coupled to the electronic system. For  $T \gtrsim 50$  K, except for a range of 35 K around  $T_{LT}$ , the magnetization recovery is well fit by the standard expression for magnetic relaxation of the central transition of a spin 7/2 nucleus with a single component  $T_1$  [18]. Between 125 K and 160 K and for  $T \lesssim 50$  K, the magnetization recovery was fit with the stretched exponential form:  $M(t) = M_0[1 - 2e^{-(t/T_1)^{1/2}}]$ , where  $M_0$  is the equilibrium magnetization. This expression represents the magnetization recovery for a distribution of relaxation rates, with a peak at  $1/6T_1$ . The data for  $^{139}T_1^{-1}$  are shown in Fig. 1. The peak at 135 K reflects the LTT transition, where the spin lattice relaxation is dominated by quadrupolar components [19].

Recently, Suh and coworkers [13] demonstrated that

TABLE I. Parameters describing distribution of activation energies:  $P(E_a) = \mathcal{N} \exp[-(E_a - E_0)^2/2\Delta^2]$ . Fits (see Fig. 1) were performed with fixed  $\tau_{\infty} = 0.03$  ps.

Material	Ref.	$E_0/k_B$ (K)	$\Delta/k_B$ (K)
$La_{1.65}Eu_{0.2}Sr_{0.15}CuO_4$		73	84
$La_{2}Cu_{0.981}Li_{0.019}O_{4}$	[22]	119	64
$La_{1.986}Sr_{0.014}CuO_4$	[11]	62	80
$\underline{La_{1.785}Eu_{0.2}Sr_{0.015}CuO_{4}}$	[13]	75	38

the strong low temperature peak in  $^{139}T_1^{-1}$  is accurately described by the Bloembergen, Purcell and Pound mechanism (BPP) [20] introduced to explain nuclear spin relaxation that results when the characteristic electron spin fluctuation frequency  $(\tau_c^{-1})$  decreases continuously with decreasing temperature:  $\tau_c = \tau_\infty \exp(E_a/k_BT)$ . The relaxation rate is given by the spectral density of fluctuations (typically a Lorentzian) evaluated at the Larmor frequency  $\omega_L$  [21]:

$$1/T_1 = \gamma^2 h_0^2 \tau_c / (1 + \omega_L^2 \tau_c^2), \tag{1}$$

where  $h_0$  is the local field fluctuating at the nuclear site, and  $\gamma$  is the gyromagnetic ratio. Hence, the peak occurs at the temperature where the continuously slowing characteristic frequency matches the measurement frequency:  $\tau_c^{-1} = \omega_L$ . Since the peak temperature is inherently probe-frequency dependent the dynamics are best described by  $E_a$ . A crucial difference from the standard BPP model is that a distribution of  $E_a$ is required to describe the relaxation data. Roughly speaking, the high temperature side of the peak in  $^{139}T_1^{-1}$  determines the center of the distribution, while the slow decrease of  $^{139}T_1^{-1}$  on low temperature side can only be explained if some fraction of the sample experiences much smaller values of  $E_a$ . We choose a Gaussian as a convenient distribution of activation energies:  $P(E_a) = \mathcal{N} \exp[-(E_a - E_0)^2/2\Delta^2]$ , where  $\mathcal{N}$  is a normalization factor; we now consider  $^{139}T_1^{-1}$  to be a function of position describing relaxation in some region of space at a particular time. This gives rise to a distribu-From Spiral and the state of the first spiral and the spiral and in Fig. 1 is a fit to this expression.

To explore the dependence of this inhomogeneous distribution of magnetic properties on impurity disorder we show  $^{139}T_1^{-1}$  results from several systems in Fig. 1: the same Eu-doped cuprate with an order of magnitude lower hole doping: La<sub>1.785</sub>Eu<sub>0.2</sub>Sr<sub>0.015</sub>CuO<sub>4</sub> [19]; lightly in-plane doped La<sub>2</sub>Cu<sub>.98</sub>Li<sub>.02</sub>O<sub>4</sub> [22]; and the Chou results [11]: La<sub>1.982</sub>Sr<sub>0.018</sub>CuO<sub>4</sub>. The evident similarity of the low temperature relaxation data is confirmed by the similar distributions of  $E_a$  (see Table 1). This indicates that impurity disorder is not the crucial element for this inhomogeneity, rather it appears intrinsic.

We observe the same wipeout of Cu signal intensity (see Fig. 2) discussed extensively by Hunt et al. [10]. A is proportional to N/T, where N is the number of nuclei, and T is the temperature, therefore  $N \sim AT$  is proportional to the number of nuclei which give rise to the NMR signal. In Fig. 2 we show N(T) for Cu and La in various fields and orientations in La<sub>1.65</sub>Eu<sub>0.2</sub>Sr<sub>0.15</sub>CuO<sub>4</sub>. About 96% of the signal from the Cu nuclei vanishes between 90 and 4 K, whereas none of the La signal is lost. The Curie-Weiss broadening of the spectra is typical for planar Cu in cuprates, however the spectra lose intensity uniformly, and develop no anomalous features. An apparent loss

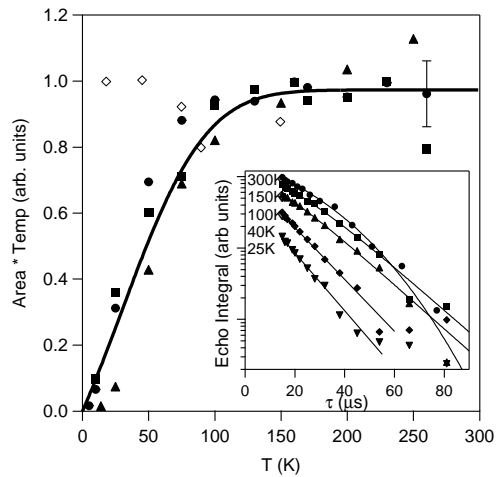


FIG. 2. NMR measurements in La<sub>1.65</sub>Eu<sub>0.2</sub>Sr<sub>0.15</sub>CuO<sub>4</sub> showing the wipeout of Cu signal. The solid symbols represent Cu data: (squares) 77 MHz,  $H_0 \perp c$ ; (circles) 86 MHz,  $H_0 \perp c$ ; (triangles) 95 MHz,  $H_0 || c$ . The open diamonds represent La data for  $H_0 || c$  at 35.9 MHz. The solid line is a plot of  $I_0(T)$  as described in the text with  $\kappa$ =1.5. Inset:  $H_0 || c$  <sup>63</sup>Cu echo size versus the pulse spacing  $\tau$  is plotted for a series of temperatures. The fits (solid lines) are described in the text.

of signal due to a shift of intensity to another region of the spectrum can be ruled out. A field dependent study revealed no evidence for a component with a different magnetic shift. Even a large change in the local NQR frequency would be easily detected in the frequency of the NMR central transition, where the quadrupolar shift is second order (i.e., a 10 MHz change in  $\nu_Q$  would shift the central transition by  $\sim 1{\text -}2$  MHz). However, the temperature dependence of the  $H_0 \perp c$  quadrupolar shift with  $H_0 \sim 80$  kG reveals no change in  $\nu_Q$  with temperature down to 4 K. Therefore the evidence suggests that the loss of intensity is not due to an inhomogeneity in either the local magnetic shift or the electric field gradient.

Rather, the slow spin fluctuations responsible for the strong low temperature peak in  $^{139}T_1^{-1}$  straightforwardly explains the intensity data if we realize that the hyperfine field  $h_0$  of the electronic moments is two orders of magnitude larger at the Cu site than it is at the La site (see Eq. 1). Thus for nuclei experiencing slow fluctuations,  $\tau_c > \tau_{\infty} e^{\kappa}$  the nuclei relax so fast the spin echo signal has decayed before it can be measured;  $\kappa$  is a constant determined by the recovery time  $t_r \simeq 15 \,\mu \text{sec}$  of the spectrometer following a spin-echo excitation pulse. The echo decay of a Cu nucleus experiencing a particular local fluctuation time  $\tau_c$  is given by:  $M_0 \exp[-t/T_{2R} - t^2/2T_{2G}^2]$ , where  $T_{2R}^{-1} = (\beta + R)^{63}T_1^{-1}$  is the Redfield term [21], and  $T_{2G}$  is the Gaussian part of the echo decay assuming static neighbors. Here  $\beta = 3$  and R is the  $T_1$ anisotropy ratio. Since  $\tau_c$  is distributed,  $^{63}T_1^{-1}$  is as well. Intensity is determined by extrapolating the spin echo decay data (available for  $t > 2t_r$ ) to t = 0; this extrapolation is dominated by the Redfield term, so we ignore the Gaussian contribution in the following discussion. The full signal from all of the nuclei is then given by:  $M(t) = \int M_0 \exp[-t/T_{2R}(\tau_c)]P(\tau_c)d\tau_c$ , where  $P(\tau_c)d\tau_c = P(E_a)dE_a$ . For  $T \gg E_0/k_B$ , M(t) decays exponentially with the single time constant  $T_2(\tau_c = \tau_\infty)$ . For  $T \lesssim E_0/k_B$  some regions relax rapidly causing M(t)to drop sharply for short t; single exponential behavior is then recovered at longer t. One can show that the extrapolated intensity  $I_0(T) = \int_0^{\kappa k_B T} P(E_a) dE_a$ , where  $\kappa \equiv \ln(\tau_{\rm cut}/\tau_{\infty})$ . For  $\tau > \tau_{\rm cut}$  excessive signal decay occurs for  $t \geq 2t_r$ , thus wiping out the signal [we use the criterion  $M(2t_r; \tau_{\rm cut})=1\%]$ . The measured low temperature anisotropy of  $^{139}T_1^{-1}$  [13] shows  $H_c^2\simeq 0$  hence  $R \simeq \frac{1}{2}$ . Using Eq. 1 and assuming  $A_{\rm hf} = 100 \text{ kOe}/\mu\text{B}$ (the wave vector dependence of the very slow spin fluctuations is not known) gives  $\tau_{\rm cut} = 0.13 \text{ ps} \Rightarrow \kappa = 1.5$ . In Fig. 2 we show a plot of  $I_0(T)$  using this value of  $\kappa$  and the distribution  $P(E_a)$  extracted from fits to the La  $T_1$ data; the agreement of this straightforward model with the data is good, especially given the uncertainty in parameters. This strongly indicates that Cu wipeout is not a measure of the stripe order parameter [10].

The Cu spin lattice relaxation rate,  $^{63}T_1^{-1}$ , was measured between 4 and 300 K. The inversion recovery data were fit to the standard expression for magnetic relaxation of the central transition with a single  $T_1$  [18]. The temperature dependence of  $(^{63}T_1T)^{-1}$  is shown in the inset of Fig. 1, as well as data from Ohsugi  $et\ al.$ , [17] for La<sub>1.85</sub>Sr<sub>0.15</sub>CuO<sub>4</sub>. The spin lattice relaxation rate of the Cu that contribute to the NMR signal at low temperatures reveals no unusual behavior, and is in fact quite similar to the  $(^{63}T_1T)^{-1}$  in La<sub>1.85</sub>Sr<sub>0.15</sub>CuO<sub>4</sub>. Note that  $(^{63}T_1T)^{-1}$  is identical for the two systems for T > 50 K. Below this the La<sub>1.85</sub>Sr<sub>0.15</sub>CuO<sub>4</sub> becomes superconducting at 38 K, whereas the La<sub>1.65</sub>Eu<sub>0.2</sub>Sr<sub>0.15</sub>CuO<sub>4</sub> does not.

The character of the Cu echo decay (Fig. 2 inset) also provides evidence for  $T_1$  inhomogeneity. The temperature dependence of the echo decay in the La<sub>1.65</sub>Eu<sub>0.2</sub>Sr<sub>0.15</sub>CuO<sub>4</sub> is similar to that in other cuprates, except for a distinct crossover from Gaussian to exponential decay around 100 K. In spite of the distributed Redfield contribution discussed above we would expect Gaussian behavior at large t; this is not observed experimentally. This behavior can be understood if the measured Cu nuclei are coupled to neighboring spins that experience a fast spin lattice relaxation. For like neighbors the echo decay is given by  $M(t) = M_0 \exp[-t^2 f(t/T_1)/2T_{2G}^2]$ , where  $f(x) = 8x^{-2}[5x/2 + 9e^{-x/2} - 2e^{-x} - 7]$  [23]. For infinite  $T_1$  the echo decay is Gaussian; as  $T_1$  gets shorter, the echo decay becomes exponential. The solid lines through the data in the inset of Fig. 2 are fits in which we assume  $T_1^{-1} = {}^{63}T_{1,\rm meas}^{-1} + {}^{63}T_{1,\rm extra}^{-1}$ , where the extra contribution is a variable parameter that represents the contribution of fast relaxation on the neighbors [24]. Qualitatively, these fits indicate that the observed Cu nuclei are coupled to neighbors that undergo  $T_1$  fluctuations much faster than those of the observed nuclei.

Combined, the La and Cu data reveal an inhomogeneous, glassy freezing of the spin dynamics in the heavily doped, stripe ordered systems. La relaxation demonstrates a dramatic slowing of spin fluctuations such that their characteristic frequency matches  $\omega_L \sim 5\text{--}50$  MHz around 10 K, and the data are well modeled by a distribution of activation energies. The quantitative explanation for the loss of Cu intensity from spin freezing provides a direct demonstration that the fluctuations are inhomogeneous: at any given temperature 0 < T < 100 K a T-dependent fraction of the Cu spins experience spin fluctuations so slow (see Eq. 1) that they are "invisible" while the remaining spins remain visible due to much faster spin fluctuations.

We have seen that quantitatively similar inhomogeneous freezing of spin fluctuations (that are well modeled by very similar distributions of activation energies) occurs in a variety of hole doped lanthanum cuprates containing impurities of very different character: i) lightly Sr-doped lanthanum cuprate containing only a few outof-plane impurities, ii) lightly Li-doped La<sub>2</sub>Cu<sub>1-x</sub>Li<sub>x</sub>O<sub>4</sub> where the impurities are in the CuO<sub>2</sub> planes, iii) both lightly and heavily Sr-doped La<sub>1.65</sub>Eu<sub>0.2</sub>Sr<sub>0.15</sub>CuO<sub>4</sub> where Eu co-doping adds more out-of-plane impurities and induces the LTT structure thought to pin charged stripes. The fact that the spin freezing is independent of both impurity density and the location of the impurity (in or out of the plane where the fluctuating moments and the charged stripes reside) strongly suggests that extrinsic impurities are not an essential element of the inhomogeneity, rather it appears to be an *intrinsic* response of the hole doped system to perturbation. Finally Hunt et al. have shown a similar loss of Cu intensity in  $La_{2-x}Sr_xCuO_4$  throughout the doping range  $\frac{1}{16} < x < \frac{1}{8}$  [10] further emphasizing the generality of this phenomenon. We note that loss of NMR signal has been observed previously in classical spin glass systems [25] and in stripe-ordered lanthanum nickelate [26].

Two different mechanisms have been explored in the literature in order to explain the spin freezing in the antiferromagnetic state: one involves the "cluster spin glass" and freezing of the transverse spin degrees of freedom [11]; another the loss at low temperatures of collective hole/stripe motion [22]. In the presence of frustration a Heisenberg system exhibits glassy behavior of the transverse spin components below the longitudinal ordering temperature [27], and Kivelson et al. have pointed out the role of disorder in striped systems [28]. The observed very slow spin fluctuations imply large clusters of spins (presumably frustrated by disorder) are involved. The role of charged stripes in these dynamics isn't clear. Stripe motion is certainly a mechanism for spin dynamics [22], however if the same mechanism is responsible for the inhomogeneous relaxation over the wide regime of hole density we observe, then the very weak hole density (hence stripe density) dependence of the distribution of activation energies implies stripe-stripe interactions play no role over a decade of stripe density; this seems unlikely. Because the stripes constitute anti-phase domain walls in the antiferromagnet, stripe disorder leads to severe spin disorder [6,7]. Hasselmann and Castro-Neto have pointed out that for  $x \sim 1/8$  the frustration can arise from point defects and disorder in the stripe topology [29]. The slow inhomogeneous dynamics could arise from frustrated interactions between such large clusters.

The authors thank N. Hasselmann, A. Castro-Neto and S. Kivelson for valuable discussions. The work at Los Alamos was performed under the auspices of the US Department of Energy. The work at University of Köln was supported by the Deutsche Forschungsgemeinschaft through SFB 341. M.H. acknowledges support by the Graduiertenstipendium des Landes Nordrhein-Westfalen.

- J. M. Tranquada et al., Nature, 375, 561 (1995); J. M. Tranquada et al., Phys. Rev. B 54, 7489 (1996).
- [2] V.J. Emery, S.A. Kivelson and O. Zachar, Phys. Rev. B 56, 6120 (1997); V.J. Emery and S.A. Kivelson, condmat/9809083.
- A.H. Castro Neto, Phys. Rev. Lett. 78, 3931 (1997).
- [4] J. Zaanen, Physica C 317-318, 217 (1999).
- [5] S.R. White and D.J. Scalapino, Phys. Rev. B 60, R753 (1999); Phys. Rev. Lett. 80, 1272 (1998).
- [6] S.-H. Lee and S-W. Cheong, Phys. Rev. Lett. 79, 2514 (1997).
- [7] Y. Yoshinari, P.C. Hammel and S-W. Cheong, Phys. Rev. Lett. 82, 3536 (1999).
- [8] J.M. Tranquada et al., Phys. Rev. B **59**, 14712 (1999).
- [9] M-H. Julien et al., Phys. Rev. Lett. 83, 604 (1999).
- [10] A. Hunt et al., Phys. Rev. Lett. 82, 4300 (1999).
- [11] F.C. Chou et al., Phys. Rev. Lett. 71, 2323 (1993).
- [12] V. Kataev et al., Phys. Rev. B 55, R3394 (1997); 58,
   R11876 (1998); J. Phys.: Cond. Mat. 11, 6571 (1999).
- [13] B.J. Suh et al., cond-mat/9911272.
- [14] U. Ammerahl et al., unpublished.
- [15] B. Büchner, private communication.
- [16] W. Wagener et al., Phys. Rev. B 55, R14761 (1997); W. Wagener et al., J. Magn. Mater. 545, 177 (1998).
- [17] S. Ohsugi et al., J. Phys. Soc. Jpn. 60, 2351 (1991).
- [18] A. Narath, Phys. Rev. 162, 320 (1967).
- [19] B. J. Suh et al., Phys. Rev. B 59, R3952 (1999).
- [20] N. Bloembergen, E. M. Purcell, and R. V. Pound, Phys. Rev. 73, 679 (1948).
- [21] C. P. Slichter, Principles of Magnetic Resonance, 3rd. Ed. (Springer Verlag, New York, 1990).
- [22] B. J. Suh et al., Phys. Rev. Lett. 81, 2791 (1998).
- [23] N. J. Curro, C. P. Slichter, J. Mag. Res. 130, 186 (1998).
- [24] One must also account for the fraction of unlike <sup>65</sup>Cu isotope; see Ref. [23].
- [25] M.C. Chen, C. P. Slichter, Phys. Rev. B 27, 278 (1983).
- [26] I.M. Abu-Shiekah et al., Phys. Rev. Lett. 83, 3309 (1999).
- [27] R. J. Gooding, Phys. Rev. Lett. 66, 2266 (1991).
- [28] S.A. Kivelson, E. Fradkin, V.J. Emery, Nature 393, 550 (1998).
- [29] N. Hasselmann, private communication.